

Photoluminescence measurements on phosphorus implanted silicon: Annealing kinetics of defects

Andreas Othonos

The Ontario Laser and Lightwave Research Centre, University of Toronto, 60 St. George St., Toronto, Ontario M5S-1A7, Canada

Constantinos Christofides

Department of Natural Sciences, Faculty of Pure and Applied Sciences, University of Cyprus, P. O. Box 537, CY-1678 Nicosia, Cyprus

(Received 11 January 1995; accepted for publication 20 March 1995)

Room-temperature photoluminescence measurements are performed in order to study the effect of thermal annealing on phosphorus implanted silicon wafers. Measurements are carried out at near band gap excitation with a Nd:YAG laser operating at 1.06 μm . Photoluminescence measurements are also carried out with 0.488 μm laser excitation. It was found that implantation conditions (dose and energy) and annealing temperature strongly influence the intensity of the photoluminescence signal. Contribution from the bulk silicon and the effects from the ion implantation to the photoluminescence signal are discussed. © 1995 American Institute of Physics.

I. INTRODUCTION

Ion-implantation has been a fundamental topic for several scientific groups for the last thirty years. The main disadvantages for ion implantation are the creation of several types of defects and, in the case of high doses, the amorphization of the surface.¹⁻⁴ The damage induced by ion implantation can be annihilated by thermal annealing which can recover the semiconductor crystallinity and activate the doping impurities. In addition, during this process a redistribution of the impurity atoms takes place.⁵

Photoluminescence (PL) in indirect semiconductors has been observed as early as the 1950s by Hynes *et al.*^{6,7} from recombination of electrons and holes in silicon. PL measurements could be very useful in the characterization of implanted layers and substrates since such measurements are very sensitive to defects in semiconducting crystals. These types of measurements have been used to study impurities in silicon⁷ and the radiation defects in ion implanted silicon.^{8,9} Photoluminescence studies on implanted silicon wafers dealing mostly with the defect structures were published by several authors.¹⁰⁻¹³ This article presents PL measurements which were made at room temperature in order to study the annealing kinetics of defects in phosphorus ion implanted silicon wafers.

II. EXPERIMENT

The experimental work was performed with a diode pumped Nd:YAG laser which was operating in a CW mode at 1.06 μm and an argon ion laser operating at 0.488 μm . The laser beam was directed and focused on the implanted silicon sample with a 10 cm focusing lens. A beam splitter which was placed in front of the laser allowed part of the beam to be reflected into a power meter for continuous monitoring of the power during the experiments. The pump power of the incident beam on the samples was maintained at 30 mW (~ 60 mW) for the 1.06 μm (0.488 μm) excitation throughout the experiment. The scattered luminescence in front of the sample was collected with a paraboloidal mirror

and was collimated. The signal was then directed to an FTIR spectrometer for analysis. In the case of the 1.06 μm excitation this signal passed through two notched filters which rejected the scattered light from the laser source and allowed detection of luminescence very close to the fundamental laser line. This configuration also allowed the detection of the silicon Raman phonon peak which was ~ 63 meV away from the laser line. In the case of the 0.488 μm laser line the notched filters were not necessary to reject the laser light since the detector was not sensitive below 0.800 μm . With the 0.488 μm excitation the photoluminescence signal was generated over a depth of ~ 1 μm from the surface of the sample, while the near gap excitation induced a PL signal mainly from the bulk. All PL measurements were carried out at room temperature. This work presents experimental results obtained from phosphorus implanted silicon wafers lightly doped with boron (20–25 Ω cm). These wafers were then implanted with phosphorus at various doses: $\Phi(\text{P}^+/\text{cm}^2) = 1 \times 10^{13}$ (W1); 1×10^{14} (W2); 1×10^{15} (W4); 1×10^{16} (W6); at 150 keV. Some wafers were also implanted with various energies: $E = 20$ keV (W7); 100 keV (W10), and 180 keV (W12) at constant dose of 5×10^{14} P^+/cm^2 . The phosphorus ion implantation was performed through a thin oxide layer at room temperature. Some samples were then annealed isochronically at various temperatures from 300 to 1100 $^\circ\text{C}$ for 1 h in an inert nitrogen atmosphere. After annealing the oxide overlayer was etched away and the samples were used for PL measurements.

III. RESULTS AND DISCUSSION

Figure 1 shows photoluminescence spectra obtained with 1.06 μm excitation for samples implanted at two different doses (at 150 keV) and annealed isochronically at different temperatures. The spectra appear to be broad (100 meV) which is typical of room temperature electron-hole recombination. Note that no additional maxima, which are characteristic of the added impurities (boron in the bulk and phosphorus in the layer), have been observed. The maximum which occurs around 1.1 μm is simply due to the indirect

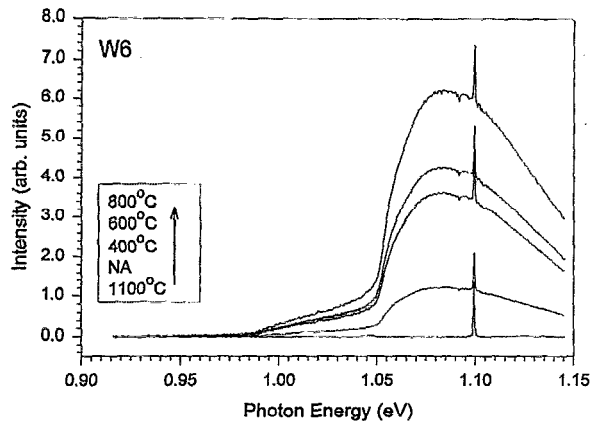
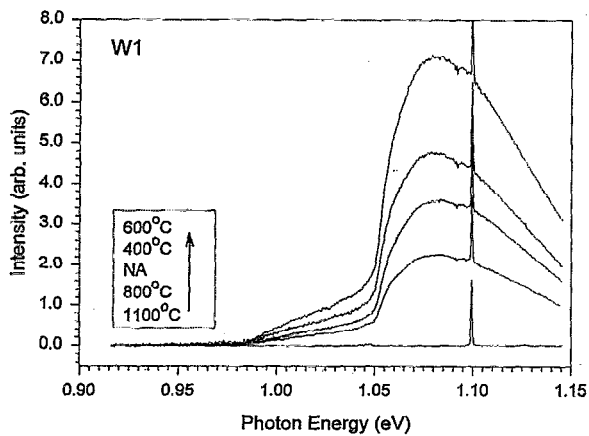


FIG. 1. Photoluminescence spectra of the phosphorus implanted silicon wafers (at 150 keV) obtained from the two extreme implanted doses Φ (P^+/cm^2): (W1) 1×10^{13} and (W6) 1×10^{16} . The excitation laser wavelength was $1.06 \mu\text{m}$ (NA: nonannealed).

transmission of electrons from the minimum to the top of the valence band involving a phonon for momentum conservation. The general shape of the curve remains the same for all annealing temperatures except at the highest temperature (1100°C). At this temperature the luminescence signal reduces to zero and the only feature that remains is a sharp peak corresponding to the Raman phonon signal from silicon.¹⁴ The main difference in room-temperature photoluminescence measurements in all the samples presented in Fig. 1 is the total integrated intensity of the signal. It appears that the various defects in the samples affect the luminescence signal.^{8,13} In this case of near-band gap excitation ($1.06 \mu\text{m}$) it is important to note that the PL signal is generated over the entire thickness of the bulk since the penetration depth at this wavelength is on the order of the sample thickness. In fact it has been shown that for this wavelength the sample is relatively transparent. Thus, the PL signal is a combination of a signal from both the bulk and the damaged implanted layer. Similarly the phonon Raman signal which is superimposed on all the PL data obtained with $1.06 \mu\text{m}$ excitation has a contribution from both the bulk and the implanted layer, with the main contribution coming from the bulk.¹⁴ It is important to point out that in order to distinguish

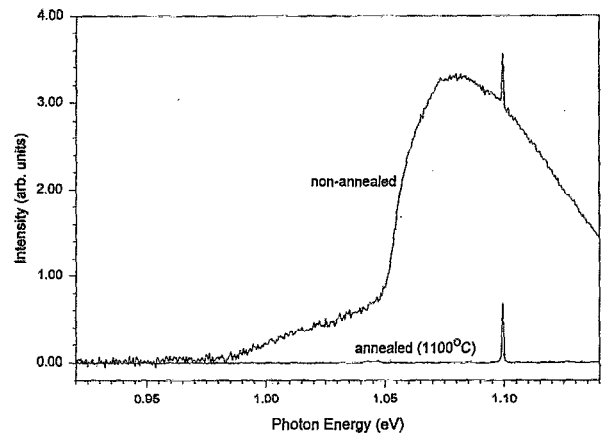


FIG. 2. Photoluminescence spectra of the nonannealed and annealed at 1100°C phosphorus nonimplanted silicon wafers. The excitation laser wavelength was $1.06 \mu\text{m}$.

the remaining defects from the implanted layer and substrates, it is necessary to work with various wavelengths.

The unexpected decrease of the photoluminescence signal at high annealing temperatures led us toward the investigation of nonimplanted samples. Figure 2 illustrates the photoluminescence signal in the case of two nonimplanted wafers (nonannealed and annealed at 1100°C). We note that an annealing at 1100°C results to zero PL signal. It seems that the induced PL signal is mainly due to the bulk. The fact that luminescence can be observed on the highly annealed ion-implanted samples indicates that thermal annealing was not totally effective in restoring crystal quality. This was also shown by Nakashima *et al.*⁸ and Svenson *et al.*⁹

Figure 3(a) shows the total integrated luminescence as a function of annealing temperature for samples implanted at doses of 1×10^{13} , 1×10^{14} , 1×10^{15} , and $1 \times 10^{16} P^+/\text{cm}^2$ at 150 keV. In this figure the integrated luminescence from the nonimplanted silicon (nonannealed) sample is taken as unity. Note that the lines joining the points are only intended to be a guide to the eye. As seen in Fig. 3(a) the nonannealed samples have a decreasing PL signal with increasing implanted dosage. It is obvious that the PL efficiency of the silicon samples deteriorates severely due to the ion-phosphorus bombardment. It is believed that the damage layer due to the implantation at the surface on the nonannealed samples caused the excited carriers to recombine non-radiatively thus reducing the luminescence normally seen from the silicon substrate. For the implanted sample series W4 which is doped at $1 \times 10^{15} P^+/\text{cm}^2$ the luminescence behavior is more complicated. At the two annealing extremes the behavior is similar to the other samples and in particular to the highest doped samples. However the luminescence has a large dip around 600°C . This phenomenon is known as negative annealing and was observed also recently while performing photothermal reflectance measurements on the same samples.¹⁵ The negative annealing around 600°C was also observed in the past by Gibbons⁵ and Vitkin *et al.*¹⁶ The PL dip at 600°C in all these cases is due to the formation of complex defects around this annealing temperature and to the fact that the majority of carriers are trapped. In the

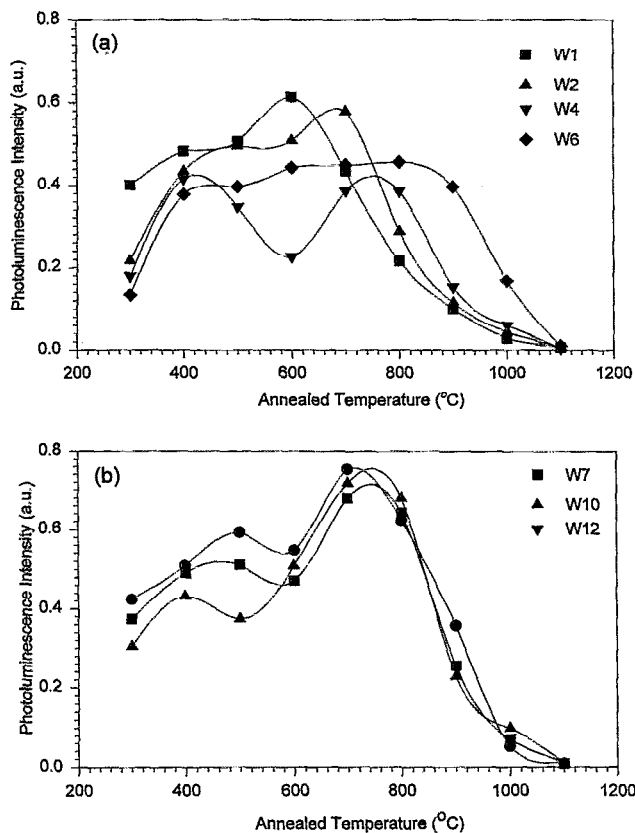


FIG. 3. Integrated photoluminescence intensity of the phosphorus implanted silicon wafers vs annealing temperature obtained from various implanted doses and energies: (a) W1, W2, W4, and W6; (b) W7, W10, and W12. The excitation laser wavelength was $1.06 \mu\text{m}$.

case, according to Pankove and Wu¹² of implantation above the amorphization dose we have the formation of clusters of 46 \AA diameter which may form centers for recombination. Looking at the data of Fig. 3(a) it appears that the curves may be divided in three well-defined annealing temperature ranges: 300–400; 400–700; and 700–1100 °C. In each stage the photoluminescence mechanism depends on the implanted induced disorder. This depends on the implantation dose since it is the dose that determines the degree of the induced disorder and amorphization. In the first range (300–400 °C) the PL signal increases drastically with annealing temperature especially for the high implanted samples. This change of the PL intensity shows the sensitivity of the PL techniques toward the annihilation of defects in this range. It is important to note that PL measurements seem very sensitive toward the defects monitoring in this range contrary to techniques such as spreading resistance measurements, Raman spectroscopy, and FTIR optical measurements as was reported by Othonos *et al.*¹⁴ and Christofides *et al.*¹⁷ In the range 400–700 °C we note that the four samples implanted at various doses present different behaviors. The PL of the sample series W1 increases with annealing temperature and reaches a maximum at 600 °C after which it decreases again. Recall that sample W1 was implanted lightly, much below the critical amorphization dose ($\Phi_c = 5 \times 10^{14} \text{ P}^+/\text{cm}^2$).¹⁸ Thus, from 300 to 600 °C at least 90% of activation of free

carriers can be achieved while the layer becomes completely recrystallized. The wafer series W2 needs an annealing of 700 °C to achieve a maximum since these samples which were implanted at a higher dose than series W1 need higher annealing for restoration of defects. It is noted that the PL of the wafer series W4 varies in a strange way with annealing temperature. The series W6 has no minimum since high implanted samples present some self-annealing phenomena (before any temperature annealing). This was also observed by Seas and Christofides¹⁵ and Ishikawa *et al.*¹⁹ This can be explained by the fact that some annihilation mechanisms take place in the case of high implantation doses which lead to self-annealing of lattice damages via the heat generated during ion implantation.³ Annealing from 700 (for W1) or 800 (for W2–W6) to 1100 °C results in a decrease of the luminescence, reaching a negligible value at the highest annealing temperature.

Figure 3(b) presents the total integrated PL signal as a function of annealed temperature for samples implanted at various energies: 20, 100, and 180 keV at a constant dose of $5 \times 10^{14} \text{ P}^+/\text{cm}^2$. For the three samples the signal reaches a maximum at 750 °C and then decreases again with increasing annealing temperature. The similar behavior of the luminescence for all three samples around this maximum seems to suggest that this feature is mainly due to the implantation rather than the lattice defects caused by implantation damage. One important observation that could be made for all samples presented in Fig. 3, is their behavior at the two different extremes of the annealed temperature which is probably due to different mechanisms for the reduction of the PL signal. The decrease of the PL of the nonannealed samples is believed to be due to the formation of defects near the surface of the samples. However, the decrease in luminescence at the highest annealing temperature is probably due to the same reason as in the reduction of luminescence of laser annealed nonimplanted silicon samples.⁸ Deep level defects were detected in laser annealed nonimplanted samples using deep level transient spectroscopy.²⁰ These deep level defects may shorten minority carriers and reduce PL intensity.

The photoluminescence signal obtained with $0.488 \mu\text{m}$ laser excitation appears to have the same spectral profile as the $1.06 \mu\text{m}$ excitation PL signal. This is not surprising since we are dealing with low-energy density excitation so that affect such as band gap renormalization or thermal affects are negligible. Figure 4(a) presents the integrated photoluminescence signal versus annealing temperature in the case where the excitation beam is $0.488 \mu\text{m}$. Clearly the photoluminescence behavior is different from the case of near-band gap excitation. We note that the PL is zero for low annealing temperatures ($<700 \text{ °C}$). The same phenomenon is also seen in Fig. 4(b) where the behavior of the PL versus annealing temperature is presented for the constant implantation samples (W7, W10, and W12). We also note that the total integrated normalized signal is smaller than the one obtained with near-band gap excitation. These differences in the PL signal may be attributed to the probing depth at $0.488 \mu\text{m}$ which is less than $1 \mu\text{m}$. This means that most of the light is absorbed near the surface, and less light reaches the bulk to induced photoluminescence signal.

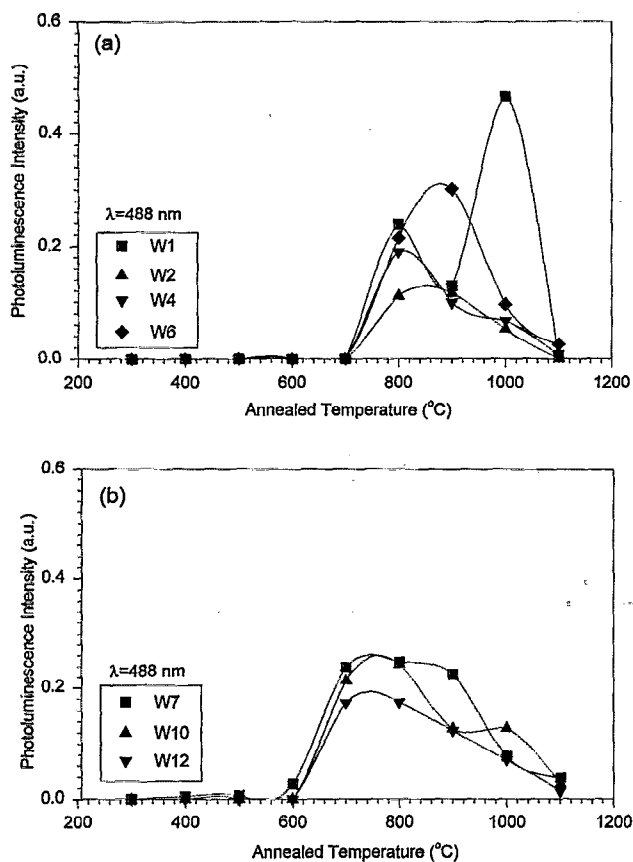


FIG. 4. Integrated photoluminescence intensity of the phosphorus implanted silicon wafers vs annealing temperature obtained from various implanted doses and energies: (a) W1, W2, W4, and W6; (b) W7, W10, and W12. The excitation laser wavelength was $0.488 \mu\text{m}$.

Figure 5(a) presents the dependence of the integrated PL intensity versus implantation dose at 150 keV. These measurements were performed with $1.06 \mu\text{m}$ laser excitation. The same behavior was also obtained by Summers and Miklosz in the case of implanted GaAs.²¹ This variation versus dose illustrated the high sensitivity of radiative recombination to damage introduced by ion implantation. In fact the PL decreases with dose. At 300°C , it seems that the PL varies almost 3 times from the lower ($1 \times 10^{13} \text{P}^+/\text{cm}^2$) to the highest dose ($1 \times 10^{16} \text{P}^+/\text{cm}^2$). This sensitivity is higher than the one presented by Seas and Christofides using photothermal reflectance measurements on the same sample.¹⁵ Figure 5(b) presents the integrated photoluminescence signal as a function of implantation energy at a constant dose. We note that PL decreases with increasing implantation energy and this can be correlated with the increase in overlap as the ion range increase. This is in agreement with the results presented by Summers and Miklosz in the case of implanted GaAs.²¹

The PL spectra obtained with the $1.06 \mu\text{m}$ excitation coincided with the silicon phonon peak. Therefore, one is able to observe simultaneously the PL and Raman signals from the same area and the same excitation probe. The combination of PL information with Raman data²² could make this a very powerful nondestructive technique for characterizing semiconductor materials. Due to the large penetration

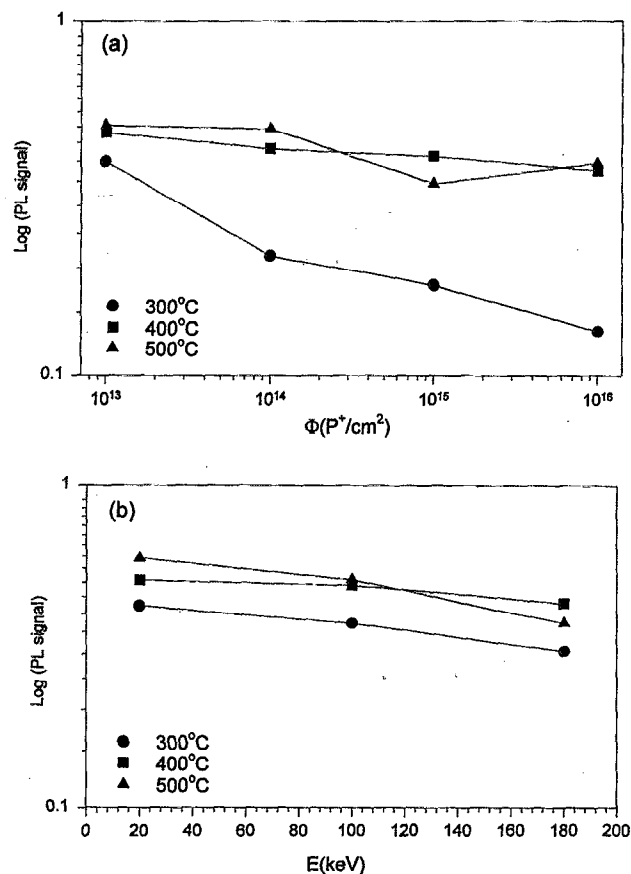


FIG. 5. Photoluminescence integrated intensity vs implantation (a) dose and (b) energy.

depth at the $1.06 \mu\text{m}$ excitation wavelength (of the order of the sample thickness 1mm), the Raman information was not very useful in our case. However, with the appropriate notched filters and detector, one will be able to observe both Raman and luminescence with excitation laser wavelength that has a short penetration depth ($\sim 1 \mu\text{m}$, which is of the order of ion implantation depth). Furthermore, measurements obtained with a series of excitation wavelengths at penetration depths ranging from sub-ion implantation depth to much greater depths will give invaluable information regarding ion implantation kinetics.

It is believed that photoluminescence has a great potential as a characterization technique for implanted materials. Its nondestructive nature and simplistic experimental arrangement, make it an ideal method for "on line" monitoring of semiconductors as they are processed. In addition the ability to obtain depth information by simply changing the wavelength of the probing beam makes this technique even more powerful.

IV. CONCLUSION

In conclusion, it has been shown that the photoluminescence measurements at room temperature can provide non-destructive information concerning the annihilation of de-

fects in the implanted layer as well as in the bulk of the silicon wafers. Three main results of this study can be summarized as follows:

- (1) The annealing temperature influences strongly the photoluminescence.
- (2) The total photoluminescence signal is a contribution from the bulk and the amorphization layer.
- (3) The photoluminescence signal is highly influenced by the implantation dose and energy.

Finally it is also important to point out that quantitative analysis of the photoluminescence signal can only be made in the case of crystalline materials. In the case of implanted (noncrystalline) materials a quantitative analysis is not an easy task. Thus, the publication of qualitative results on this topic will help considerably in the effort to establish in the future the way for photoluminescence quantitative analysis.

¹H. Ryssel and I. Ruge, *Ion Implantation* (Wiley, New York, 1986).

²C. Christofides, *Semicond. Sci. Technol.* **7**, 1283 (1992).

³J. F. Gibbons, *Proc. IEEE* **56**, 295 (1968).

⁴C. Christofides, G. Ghibaud, and H. Jaouen, *J. Appl. Phys.* **65**, 4840 (1989).

⁵J. F. Gibbons, *Proc. IEEE* **60**, 1062 (1972).

⁶J. R. Haynes and H. B. Briggs, *Phys. Rev.* **86**, 647 (1952).

⁷J. R. Haynes and W. C. Wesphal, *Phys. Rev.* **101**, 1676 (1956).

⁸H. Nakashima, Y. Shiraki, and M. Miyao, *J. Appl. Phys.* **50**, 5966 (1979).

⁹O. F. Swenson, T. E. Luke, and R. L. Hengehold, *J. Appl. Phys.* **54**, 6329 (1983).

¹⁰C. G. Kirkpatrick, J. R. Noonan, and B. G. Streetman, *Radiat. Eff.* **30**, 97 (1976).

¹¹J. R. Noonan, C. G. Kirkpatrick, and B. G. Streetman, *Radiat. Eff.* **21**, 225 (1974).

¹²J. I. Pankove and C. P. Wu, *Appl. Phys. Lett.* **35**, 937 (1979).

¹³H. Nakashima and Y. Shiraki, *Appl. Phys. Lett.* **33**, 257 (1978).

¹⁴A. Othonos, C. Christofides, J. Boussey-Said, and M. Bisson, *J. Appl. Phys.* **75**, 8032 (1994).

¹⁵A. Seas and C. Christofides, *Appl. Phys. Lett.* (to be published).

¹⁶I. A. Vitkin, C. Christofides, and A. Mandelis, *Appl. Phys. Lett.* **54**, 2392 (1989).

¹⁷C. Christofides, A. Othonos, M. Bisson, and J. Boussey-Daid, *J. Appl. Phys.* **75**, 3377 (1994).

¹⁸S. Prussin, D. Margolese, and R. Tauber, *J. Appl. Phys.* **57**, 180 (1985).

¹⁹K. Ishikawa, M. Yoshida, and M. Inqe, *Jpn. J. Appl. Phys.* **26**, L1089 (1981).

²⁰P. M. Mooney, R. T. Young, J. Karins, Y. H. Lee, and J. W. Corbett, *Phys. Status Solidi A* **48**, K31 (1978).

²¹C. J. Summers and J. C. Miklosz, *Appl. Phys. Lett.* **44**, 4653 (1973).

²²A. Othonos and C. Christofides (unpublished).